

Morphological and ultrastructural characterization of the acidophilic and lipid-producer strain *Chlamydomonas acidophila* LAFIC-004 (Chlorophyta) under different culture conditions

Luana dos S. Souza¹ · Carmen Simioni² · Zenilda L. Bouzon³ ·
Rosana de Cassia da S. Schneider⁴ · Pablo Gressler¹ · Maria Cecília Miotto¹ ·
Marcio J. Rossi⁵ · Leonardo R. Rörig⁶

Received: 10 May 2016 / Accepted: 20 September 2016 / Published online: 30 September 2016
© Springer-Verlag Wien 2016

Abstract *Chlamydomonas acidophila* LAFIC-004 is an acidophilic strain of green microalgae isolated from coal mining drainage. In the present work, this strain was cultivated in acidic medium (pH 3.6) under phototrophic, mixotrophic, and heterotrophic regimes to determine the best condition for growth and lipid production, simultaneously assessing possible morphological and ultrastructural alterations in the cells. For heterotrophic and mixotrophic treatments, two organic carbon sources were tested: 1 % glucose and 1 % sodium acetate. Lipid content and fatty acid profiles were only determined in phototrophic condition. The higher growth rates were achieved

in phototrophic conditions, varying from 0.18 to 0.82 day⁻¹. Glucose did not result in significant growth increase in either mixotrophic or heterotrophic conditions, and acetate proved to be toxic to the strain in both conditions. Oil content under phototrophic condition was 15.9 % at exponential growth phase and increased to 54.63 % at stationary phase. Based on cell morphology (flow cytometry and light microscopy) and ultrastructure (transmission electron microscopy), similar characteristics were observed between phototrophic and mixotrophic conditions with glucose evidencing many lipid bodies, starch granules, and intense fluorescence. Under the tested conditions, mixotrophic and heterotrophic modes did not result in increased neutral lipid fluorescence. It can be concluded that the strain is a promising lipid producer when grown until stationary phase in acidic medium and under a phototrophic regime, presenting a fatty acid profile suitable for biodiesel production. The ability to grow this strain in acidic mining residues suggests a potential for bioremediation with production of useful biomass.

Handling Editor: Peter Nick

✉ Luana dos S. Souza
luanass1981@hotmail.com

- ¹ Post Graduate Program in Biotechnology and Biosciences, Federal University of Santa Catarina, 88049-900, CP 476 Florianópolis, SC, Brazil
- ² Postdoctoral Research of Post-Graduate Program in Cell Biology and Development, Department of Cell Biology, Embryology and Genetics, Federal University of Santa Catarina, 88049-900, CP 476 Florianópolis, SC, Brazil
- ³ Central Laboratory of Electron Microscopy, Federal University of Santa Catarina, 88049-900, CP 476 Florianópolis, SC, Brazil
- ⁴ Department of Chemistry and Physics, Graduate Program in Environmental Technology, University of Santa Cruz do Sul, 96815-900 Santa Cruz do Sul, RS, Brazil
- ⁵ Bioprocess Laboratory, Department of Microbiology and Parasitology, Federal University of Santa Catarina, 88049-900, CP 476 Florianópolis, SC, Brazil
- ⁶ Phycology Laboratory, Botany Department, Federal University of Santa Catarina, 88049-900, CP 476 Florianópolis, SC, Brazil

Keywords Flow cytometry · Ultrastructure · Lipid bodies · Mixotrophy · Heterotrophy · Fatty acids

Introduction

Microalgae are fast-growing photosynthetic microorganisms capable of generating biomass rich in several primary metabolites, such as proteins and lipids, as well as secondary metabolites, with a wide range of applications. The high quantity and quality of some of these molecules have stimulated the production of high-value products, including human health food, animal feed, biofuels, fine chemicals, and

pharmaceuticals (Spolaore et al. 2006; Bux 2013; Richmond and Hu 2013).

One of the most promising uses of microalgal biomass is the production of biofuels. This can be achieved in three general ways: (1) direct production of microalgae to recover fuel molecules (e.g., ethanol, hydrogen and alkanes) without the need for extraction, (2) processing full microalgal biomass for fuel production, and (3) production of microalgal extracts to generate fuel molecules (USDOE 2010). In the third case, lipids are the main type of molecules prospected, and can be used as biodiesel through transesterification (Chisti 2007). The most important microalgae groups as a source of lipids are the chlorophytes and the diatoms (Sheehan et al. 1998). The levels of lipids in these microalgae are around 30 %, but the yield can be increased in some species by manipulating environmental conditions, especially by imposing stress, such as nutrient starvation, temperature (low, high) shift, changes in salinity and pH, light or UV irradiation (low, high), among others (Sharma et al. 2012).

The massive production of microalgal biomass is, in part, limited by the sensitivity of many species to environmental variations and competition with invasive species, which diminish the productivity of commercial algal processing. In this sense, extremophilic microalgae (e.g., acidophilic) have gained interest because of their ability to grow in extreme conditions, excluding eventual competitors, producing high-value compounds, while acting as a remediator of effluents (e.g., absorption/adsorption of heavy metals) (Inthorn 2001; Eibl et al. 2014; Kumar et al. 2015; Varshney et al. 2015). Microalgae groups are characterized by high morphophysiological and biochemical diversity. Although they are preferably phototrophic, some microalgae species are able to grow in the absence of light, consuming soluble organic molecules, such as sugars, organic acids, and acetate (heterotrophy). In the mixotrophic regime, CO₂ and organic carbon are assimilated, and both metabolisms, heterotrophic and photosynthetic, operate simultaneously (Perez-Garcia et al. 2011). In fact, several authors have recently reported a significant increase in biomass, carbohydrates, and lipid contents of some microalgae species under mixotrophic and heterotrophic conditions when compared to phototrophic conditions (e.g., Liang et al. 2009; Liu et al. 2011; Giovanardi et al. 2013; Liang 2013; Liu et al. 2014; Rattanapoltee and Kaewkannetra 2014). In this case, enhanced lipid production is not related to stress, but to the effect of the organic carbon source (e.g., glucose) in Calvin Cycle, leading to a lower consumption of cofactors (e.g., ATP) and to a more economical formation of Acetyl CoA, the precursor of fatty acids (Xiong et al. 2010). Therefore, the ability to grow microalgae in extreme conditions and under heterotrophic or mixotrophic conditions represents a strategic line of research.

In algae and plants, the de novo synthesis of lipids uses carbon molecules photosynthetically fixed as substrate

(e.g., 3-phosphoglycerate). Two large groups of lipids are synthesized in cells: polar and neutral. Polar lipids are major components of biological membranes, and neutral lipids are energy-rich compounds often stored in cytosolic lipid bodies consisting of triacylglycerides (TAG), sterols, sterol esters, monoglycerides (MAG), and diglycerides (DAG) (Harwood and Jones 1989; Li et al. 2010; Radakovits et al. 2010).

Detecting the production of neutral lipids is a challenge in biofuel research (Lee et al. 1998). However, combining flow cytometry with a fluorescent dye is highly effective for rapidly selecting and isolating strains of microalgae producing high levels of neutral lipids by the small quantities of biomass required (Montero et al. 2011; Guzman et al. 2012; Cirulis et al. 2012; Roleda et al. 2013; Velmurugan et al. 2013; Saltpati and Pal 2014; Wu et al. 2014).

Understanding the metabolism of species and strains of microalgae is critical to the successful development of cultivation and production processes (Trainor 2009). However, data on the formation and mobilization of lipid bodies at the subcellular level and the regulation of these processes are still scarce (Přibyl et al. 2012). Therefore, to expand this knowledge in the present study, light, confocal, and electron microscopy, as well as flow cytometry were used to characterize the physiological and morphological responses of an acidophilic, lipid-producing strain of *Chlamydomonas acidophila* LAFIC-004 cultivated under phototrophic, mixotrophic, and heterotrophic conditions. Based on indications from literature, we hypothesize that this acidophilic strain could grow better under mixotrophic and heterotrophic conditions than in phototrophic conditions, increasing its content of lipids.

Material and methods

Microalgae strain and culture conditions

The acidophilic strain of *C. acidophila* LAFIC-004 was isolated from acidic coal mining drainage (AMD) in the Criciúma region of Santa Catarina State in southern Brazil (latitude 28°35'40.73"S, longitude 49°27'37.98"W) and held in the Microalgae Culture Collection of the Phycology Laboratory (MCC-LAFIC) at the Federal University of Santa Catarina (UFSC). The strain was cultured in Modified Acid Medium (MAM, Olavenson and Stoke 1989), pH 3.6, irradiance of 50 $\mu\text{mol}\cdot\text{m}^{-2}\cdot\text{s}^{-1}$ (fluorescent lamps), photoperiod of 12 h, and temperature of 22 ± 2 °C. The formulation of MAM was (in $\text{g}\cdot\text{L}^{-1}$) (NH₄)₂ SO₄ 0.5, CaCl₂·2H₂O 0.01, MgSO₄·7H₂O 0.5, KH₂PO₄ 0.3, NaCl 0.03, Na₂-EDTA 0.01, (in $\text{mg}\cdot\text{L}^{-1}$) FeSO₄·7H₂O 4.98, H₃BO₃ 2.86, MnCl₂·4H₂O 1.81, ZnSO₄·5H₂O 2.22, NaMoO₄·2H₂O 0.39, CuSO₄·5H₂O 0.079, Co(NO₃)₂·6H₂O 0.0494, biotin 1.0, B₁₂ 10.0, and thiamine 20.0. The pH was adjusted to 3.6 with sulfuric acid.

These growing conditions were defined as standard culture conditions for the strain.

Growth pattern of *C. acidophila* LAFIC-004 at standard culture conditions

Several growth experiments with *C. acidophila* LAFIC-004 were performed to assess the time of growth phases (exponential and stationary), as well as the exponential growth rate under standard phototrophic conditions, and to generate biomass for lipid analyses. These experiments were conducted in three to five replicates in flasks of 250 mL or 5000 mL with 10 % v/v of inoculum consisting of an exponentially growing culture of the strain. During the growth period, samples from these flasks were collected every 1 to 3 days for instant cell enumeration with Neubauer hemocytometer. Exponential and stationary phase were defined visually on the growth curve. Exponential growth rate (μ) was calculated according to Eq. 1, where De_0 is cell density (cells.mL⁻¹) at the beginning of exponential phase, De_t is cell density at the end of exponential phase, and t is elapsed time (days) between De_0 and De_t .

$$\mu = \frac{(\ln De_t - \ln De_0)}{t} \quad (1)$$

Growth of *C. acidophila* LAFIC-004 at different conditions

Cultivation experiments were conducted to evaluate and compare the growth characteristics of the strain under phototrophic, mixotrophic, and heterotrophic conditions. Cultivation conditions were as follows: (a) phototrophic (Photo), standard conditions described above; (b) mixotrophic with 1 % glucose (Mix-Glu); (c) mixotrophic with 1 % acetate (Mix-Acet); (d) heterotrophic with 1 % glucose (Het-Glu); and (e) heterotrophic with 1 % acetate (Het-Acet). The tests were performed in triplicate using 250 mL flasks containing 150 mL of sterile culture medium and 10 mL of an axenic inoculum with cell density of approximately 4×10^6 cells.mL⁻¹. Flasks of mixotrophic treatments were exposed to the same photoperiod and irradiance as those in phototrophic mode. Flasks of heterotrophic treatments were sealed with aluminum foil. All other culture variables were equal to the standard conditions already described. Glucose and acetate concentrations were used as defined by Moon et al. (2013). In each flask, cell density was determined by Neubauer hemocytometer at the time of inoculation (D_0) and at the supposed end of exponential phase (D_f), as defined in the initial growth experiments under phototrophic conditions (see above). A relative growth rate was then generated by the percentage increase in cell density (cells.mL⁻¹) along the incubation time, according to Eq. 2, where D_0 is cell density at the initial time, D_f is cell density at

final time, and Te is elapsed time (days). This equation was modified from Kain (1987) and is commonly used in the estimation of growth rates of macroalgae using dry weight, but it was adopted here for microalgae using cell density, replacing the equation of exponential growth, essentially because cell density data were available only at the beginning and end of the experiment. Generating a growth curve with daily data is difficult in axenic cultures because of the requirement of daily removal for sampling could cause contamination.

$$\% \text{ increase} = 100 \left[\left(\frac{D_f}{D_0} \right)^{1/Te} - 1 \right] \quad (2)$$

Samples from Photo, Mix-Glu, Het-Acet, and Het-Glu treatments were collected at the end of the experiment for morphological analysis by flow cytometry (size, complexity, and presence of neutral lipids), light microscopy (LM), confocal microscopy (CM), and transmission electron microscopy (TEM). Mix-Acet treatment showed no growth, making it impossible to perform these analyses.

Lipid extraction and fatty acid analysis

It was determined the oil content and fatty acid profile in the standard phototrophic condition described above. The analyses were performed on the exponential and stationary growth phase as defined according to the growth curves from “Growth pattern of *C. acidophila* LAFIC-004 at standard culture conditions” section. The extraction and determination of lipid content was performed by gravimetry according to the method of Bligh and Dyer (1959), using 1 g of lyophilized biomass. Analysis was performed in triplicates. The oils were converted to fatty acid methyl esters (FAME) by heating with BF₃-MeOH, as recommended by the AOCS standard methodology (Christie 1989). The esters were extracted with heptane and dried over anhydrous Na₂SO₄.

The chromatographic analysis was performed in a Shimadzu QP 2010 Plus gas chromatograph (GC) equipped with an AOC 20i Automatic Injector coupled to Mass Spectrometry (CG-EM). The method used was AOCS Ce 1c-89 (AOCS 2006). The heating conditions of the DB5 ms column (30 m × 0.25 mm × 0.25 μm) were 150 °C (0.1 min) heating to 250 °C (3 °C.min⁻¹) and then continuing heating at 30 °C.min⁻¹ to 300 °C. In the mass detector, the temperature of the ionization source (electron impact, EI) and the interface temperature were both 280 °C. The injection system was used in split mode (1:5) at 250 °C, and the mass detector was maintained in the scan mode. Helium was used as the carrier gas at a flow rate of 1.0 mL.min⁻¹. The methyl ester standards (Sigma ©) were injected along with the samples in triplicate in 1 μL aliquots.

Cell morphology analysis

For cell morphology analysis, live samples were analyzed and photographed with an Olympus BX 41 epifluorescence microscope equipped with a QCapture Software Pro 5.1 image capture system. For visualization of neutral lipids, samples were incubated with Nile Red—NR (9-diethylamino-5Hbenzo [α] phenoxazine-5-one; Sigma-Aldrich, St. Louis, MO, USA) diluted in DMSO (0.25 mg.mL^{-1}). Ten microliters of the stock solution were added into 2 mL of the cell suspension, mixed by vortexing, and then kept in the dark for 30 min. NR fluorescence was observed under confocal laser scanning microscopy (Leica DMI 6000 B) at 470 nm laser excitation with emission spectrum from 530 to 630 nm (Saltpati and Pal 2014). Chloroplast autofluorescence was observed at 488 nm laser excitation with emission spectrum from 650 to 750 nm (Zitta et al. 2013). One to three microscope slides of each test flask (treatment replicate) were made to observe and photograph the cells totaling 300 to 800 cells analyzed from each flask.

Detection of lipids, cell size, and complexity by flow cytometry

Cell suspensions from the different treatments containing 10^6 cells. mL^{-1} were stained with NR stock solution in a manner similar to that described above for cell morphology. Fluorescence read out was obtained using an excitation of 488 nm with an argon laser. The emission signal was measured in two channels under excitement: frontal fluorescence (FSC Forward Scatter) and lateral (SSC Side Scatter) through the detectors FITC (green fluorescence; 530/40 nm) and PE (orange fluorescence; 580/30 nm), indicative of pigments (carotenoids, chlorophyll) and neutral lipids, respectively, in the cells stained with NR. A cell suspension sample without the addition of NR dye was also analyzed in the flow cytometer for identification and characterization of cell populations through measures of size FSC (Forward Scatter) and complexity SSC (Side Scatter). For each event, 200,000 cells were analyzed automatically by the equipment. The fluorescence intensity was expressed as arbitrary units (a.u.), and the images were analyzed using the software Flowing ver. 2.5.1.

Cell ultrastructure analysis

TEM was performed according to the method of Bouzon et al. (2005) and Simioni et al. (2014). Samples were fixed with 2.5 % glutaraldehyde in sodium cacodylate buffer 0.1 M (pH 7.2) for 4 h at 4 °C. Thereafter, fixed samples were washed four times with sodium cacodylate buffer 0.1 M (pH 7.2) for 10 min. The material was post-fixed with 1 % osmium tetroxide (OsO_4) and 0.1 M sodium cacodylate buffer (pH 7.2) for 2 h at room temperature. Then, three washes of 10 min each were performed in 0.1 M sodium cacodylate

buffer. After washes, the samples were dehydrated in a growing series of acetone *v/v* (30, 50, 70, 90, and 100 %), 15 min each step. The final series of 100 % acetone was performed twice. The material was then infiltrated with Spurr's resin in graded series of acetone-Spurr's resin for 3 days, followed by two infiltrations with pure resin for 12 h, and finally polymerized in an oven at 70 °C for 24 h. The ultrathin sections (60 nm) were performed with a diamond knife on an ultramicrotome and subsequently stained with 1 % uranyl acetate for 20 min and 1 % lead citrate for 10 min. The sections were observed and photographed in a transmission electron microscope (JEM 1011; Central Laboratory of Electron Microscopy—LCME/UFSC) under acceleration of 80 kV.

Statistical analysis

The tests were performed using triplicates for each treatment. The use of three replicates for assays with this strain proved to be adequate in previous trials, since the inoculum was in exponential growth phase (healthy condition), as was the case in the present experiments, resulting in reproducible behavior. Means and standard errors were calculated for all treatments, and significant differences were determined by an analysis of variance according to Tukey's highly significant differences test ($p < 0.05$). The comparison among the treatments was performed by one-way ANOVA test ($p < 0.05$).

Results

Growth pattern of *C. acidophila* strain LAFIC-004

After isolation and purification, the strain *C. acidophila* LAFIC-004 showed rapid acclimation and satisfactory growth under standard laboratory conditions. Thirteen growth curves obtained in these conditions were used to identify the approximate times for exponential and stationary growth phases of the strain (Table 1). Exponential phases lasted up to 13 days after inoculation and stationary phases extended to 30 days after inoculation. Based on these data, the typical times to exponential and stationary phases were defined to be 12 and 30 days, respectively. We chose to use the longer times obtained (curve no. 13, Table 1) assuming that they best characterize the typical biochemical state of cells in these growth phases. Flasks of curve no. 13 had a larger volume (5000 mL) and served to obtain and characterize the biomass of the strain at standard conditions.

Exponential growth rate (μ) of these cultures was then calculated with cell density data from the 3rd (De_0) and the 13th (De_{13}) days, with 10 days of elapsed time (t). Average value for μ was 0.49 day^{-1} . It is noteworthy that the pH varied by an average of only 0.3 unit in the cultures, even after

Table 1 Growth data of *C. acidophila* LAFIC-004 in Modified Acid Medium, pH 3.6 under phototrophic conditions. μ , growth rate at exponential phase. SE, standard error of the mean. All experiments performed with three to five replicates in 150 mL flasks except no. 13 which was conducted in 5000 mL flasks for biomass production and determination of lipid content and fatty acid profile

Growth curve no.	μ (day ⁻¹)	Exponential phase end (days after inoculation)	Stationary phase end
1	0.28	5	14
2	0.78	4	12
3	0.55	6	14
4	0.44	7	15
5	0.23	7	15
6	0.55	7	18
7	0.65	7	17
8	0.38	7	22
9	0.82	4	16
10	0.76	4	15
11	0.21	10	26
12	0.51	6	21
13	0.18	13	30
Mean	0.49	6.69	18.07
SE	0.06	0.70	1.46

30 days of growth, indicating the acidic buffering capacity of the culture media.

Growth of *C. acidophila* LAFIC-004 at different conditions

The growth experiments under different conditions (phototrophic, mixotrophic, and heterotrophic) were conducted until the 12th day, assuming that, at the very least, phototrophic treatments would grow exponentially, thereby avoiding the possibility of excess dead cells from growth decay. Cultivation times were equalized for all treatments to compare growth efficiency.

Cell growth was higher in the Photo treatment (% increase, 87.9), followed by Mix-Glu (% increase, 56.5), presenting significant difference between them ($p < 0.05$). Growth in heterotrophic condition was low (% increase, 12.2) with no significant difference between treatments with glucose (Het-Glu) and acetate (Het-Acet) ($p > 0.05$) (Fig. 1). No growth was observed in the Mix-Acet treatment.

Lipid content and fatty acid profile

C. acidophila LAFIC-004 showed relatively high levels of lipid production when grown under phototrophic conditions with 15.9 % in the exponential phase and 54.6 % in the late stationary phase indicating good potential as a lipid source (Fig. 2). The fatty acid profile showed considerable difference between the samples from the two growth phases (Fig. 2). The most abundant fatty acid in the oil obtained from exponential phase was hexadecanoic acid (C16:0) with 46.2 %, followed by (Z)-octadec-9-enoic acid (C18:1c) and (E)-octadec-11-enoic acid (C18:1t) with 31.4 and 14.7 %, respectively. In

the oil obtained from the late stationary phase, the percentage of hexadecanoic acid (C16:0) decreased to 20.4 %, while (Z)-octadec-9-enoic acid (C18:1c) appeared as the most abundant, with 35.7 %, followed by (9Z,12Z)-octadeca-9,12-dienoic acid (C18:2) with 22.3 % (Fig. 2). In general, in both cases, saturated and mono- or diunsaturated fatty acids were more important.

Cell morphology

When analyzed by light microscopy, the Photo-treated cells of *C. acidophila* LAFIC-004 showed spherical shape with intense green color and vacuolated regions (Fig. 3a). These characteristics were also found in the cells treated with Mix-

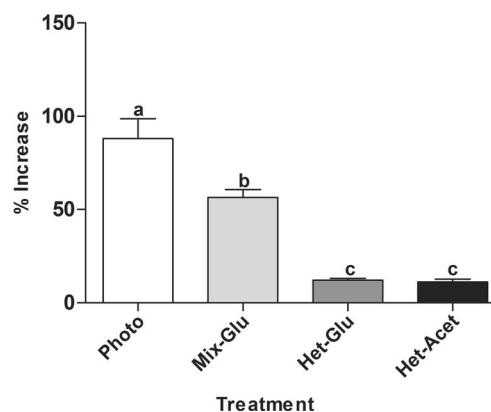


Fig. 1 Percent of increase in *C. acidophila* LAFIC-004 cells in phototrophic (Photo) and mixotrophic conditions with 1 % glucose (Mix-Glu), heterotrophic with 1 % glucose (Het-Glu), and heterotrophic with 1 % acetate (Het-Acet) treatments. Letters indicate significantly different treatments according to the Tukey multiple comparison test (mean \pm SD, $n = 3$)

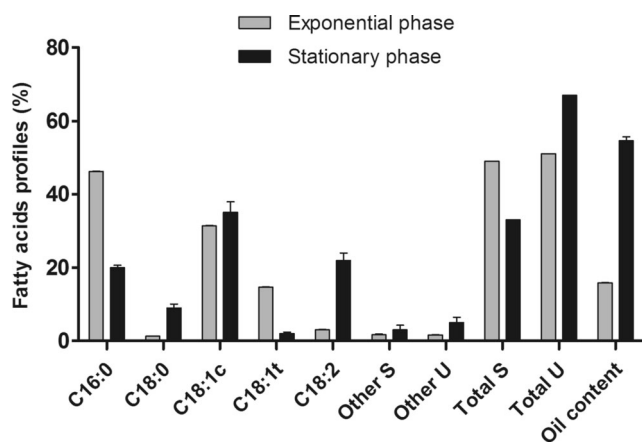


Fig. 2 Fatty acid profiles of *C. acidophila* strain LAFIC-004 from exponential growth phase (day 12) and stationary growth phase (day 30) under phototrophic conditions. *Other S* = unidentified saturated fatty acid (>2 %); *Other U* = unidentified unsaturated fatty acid (>2 %); *Total S* = total fatty acids saturated; *Total U* = total fatty acids unsaturated; *Oil content* = total oil content. Percentages are expressed as mean \pm standard deviation, $n = 3$

Glu (Fig. 3b). In Het-Glu treatment, cells showed a weak greenish color, but no vacuolated regions (Fig. 3c). In Het-Acet treatment, cells showed alterations in shape and pigmentation (Fig. 3d).

When analyzed by laser confocal scanning microscopy, cells from both Photo and Mix-Glu treatments showed intense chloroplast autofluorescence (Fig. 3e, f). In the Het-Glu treatment, cells showed a decrease in autofluorescence (Fig. 3g), and in Het-Acet treatment, cells presented little, or no, autofluorescence (Fig. 3h).

By laser confocal scanning microscopy, living cells treated with Photo and Mix-Glu and tagged with Nile Red showed yellowish punctuations, highlighting the neutral lipids (Fig. 3i, j). In Het-Glu and Het-Acet treatments, these punctuations were still visible, but fewer in number (Fig. 3k, l).

Lipid detection, cell size, and complexity by flow cytometry

Light scattering measurements of size (FSC-A) and cell complexity (SSC-A) of *C. acidophila* LAFIC-004 are presented in Fig. 4a, b, respectively. With respect to the cell size, all treatments presented statistical differences, but with regard to cellular complexity treatments, Photo and Mix-Glu showed no significant difference ($p < 0.05$); however, they were both significantly different from Het-Glu and Het-Acet treatments. Het-Glu and Het-Acet showed considerable changes in morphology and cell complexity.

Photo and Mix-Glu treatments showed a heterogeneous cell distribution (Fig. 5) with medium and large sizes and low complexity. Cells treated with Het-Glu had a more homogeneous distribution compared with Photo-treated cells which

were smaller in size and had low complexity. On the other hand, cells treated with Het-Acet showed high complexity compared to the other treatments, and most cells were small in size (Fig. 5).

NR was efficient in staining cell pigments, showing significant differences when scanned through the FITC channel (Fig. 6a). Photo treatment showed the highest fluorescence intensity, followed by Mix-Glu. Het-Acet treatment showed the lowest fluorescence intensity. These results are related to the cell density data, which revealed higher increase by Photo treatment, followed by Mix-Glu. Neutral lipids, as represented by the fluorescence intensity of treatments stained with NR and then scanned through PE channel, showed no significant difference between Photo and Mix-Glu treatments in contrast to both heterotrophic treatments (Fig. 6b). Between heterotrophic treatments, Het-Glu showed greater fluorescence than that shown by Het-Acet (Fig. 6b).

Cell ultrastructure

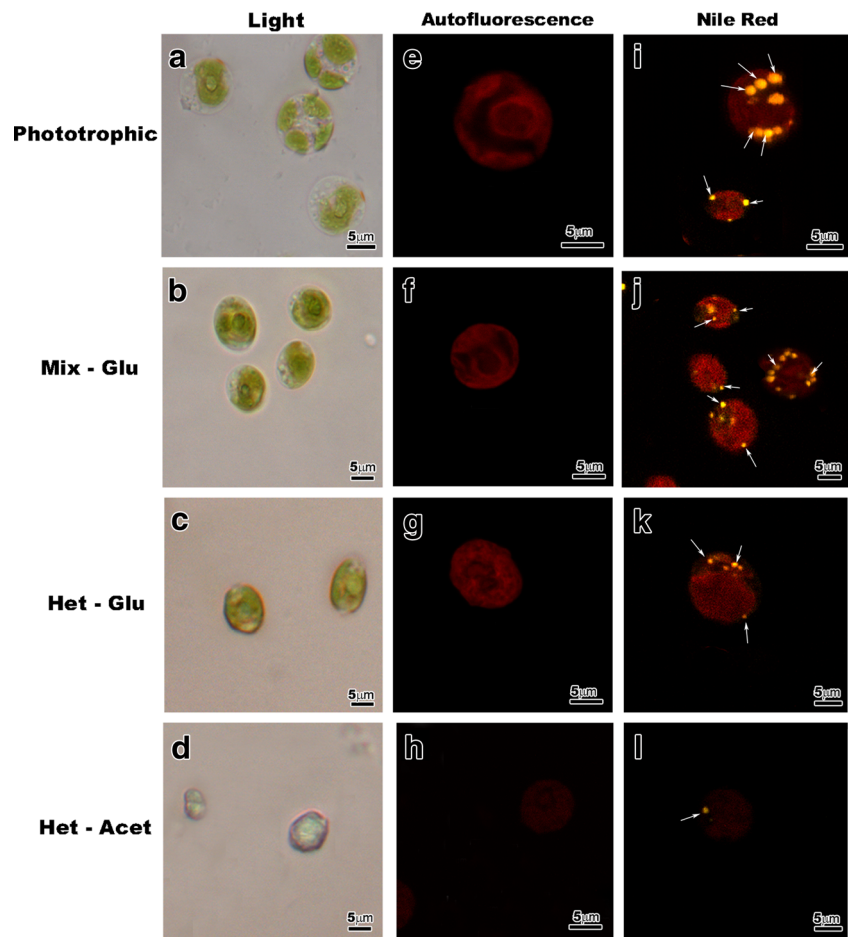
When observed under TEM, Photo-treated cells of *C. acidophila* LAFIC-004 showed a typical Chlamydomonadaceae structure with one chloroplast occupying most of the cell volume and elongated thylakoids in groups of three or four (Fig. 7a, b). Inside the chloroplast, it was possible to observe the eyespot, a carotenoid concentration region (Fig. 7c), as well as a large pyrenoid surrounded by starch grains (Fig. 7d). Additionally, several lipid bodies with peripheral electron-dense punctuations were visualized (Fig. 7e, f).

The cells of Mix-Glu treatment showed similar characteristics to those from Photo treatment, with a chloroplast occupying almost the entire cell volume and the presence of organized and elongated thylakoids, with evident pyrenoid and eyespot (Fig. 8a–d). The starch grains dispersed inside the chloroplast were observed in larger amount compared to phototrophic (Fig. 8e). Furthermore, the lipid bodies were visualized in greater quantities in this treatment, showing peripheral electron-dense punctuations (Fig. 8f).

In Het-Glu treatment, cells showed altered form, confirming observations from light microscopy, but maintaining cell organization with visible thylakoid membranes in the chloroplast (Fig. 9a, b). A decrease in the number and size of starch grains was seen around the pyrenoid (Fig. 9b, c), as well as an increase of electron-dense punctuations in lipid bodies (Fig. 9d).

Under Het-Acet treatment, dramatic changes in cell structure could be observed (Fig. 10a). The thylakoids appeared degenerated throughout the cell (Fig. 10b, c), and only a few lipid bodies and starch grains were observed. Furthermore, electron-dense punctuations appeared inside the pyrenoid, a feature not observed in the other treatments (Fig. 10d).

Fig. 3 *C. acidophila* LAFIC-004 cells under different experimental conditions of cultivation. Light microscopy (*a–d*), confocal laser scanning of autofluorescence of chloroplast (*e–h*), and tagged with Nile Red (*i–l*). Cells showed greenish coloration with regions vacuolated in phototrophic condition (*a*) and mixotrophic with 1 % glucose (*Mix-Glu*) (*b*), while in heterotrophic condition with 1 % glucose (*Het-Glu*), cell number and size are reduced (*c*), together with the absence of pigmentation in cells with heterotrophic treatment with 1 % acetate (*Het-Acet*) treatment (*d*). The autofluorescence of chloroplasts (*red*) in phototrophic (*e*) and *Mix-Glu* (*f*) cells showed intense fluorescence with intact chloroplast structure. In *Het-Glu* treatment, chloroplast appeared granular with autofluorescence (*g*), while in *Het-Acet* treatment, cells showed little fluorescence (*h*). By Nile Red staining (*yellow*) of cells in phototrophic (*i*) and *Mix-Glu* treatments (*j*), yellow punctuations (*arrowheads*) could be observed, while these punctuations are decreased in *Het-Glu* (*k*) and *Het-Acet* treatments (*l*)



Discussion

C. acidophila LAFIC-004 was easily cultivated under phototrophic conditions when maintaining culture medium pH similar to that found in its original environment (2.5–3.8).

Growth rate at the standard defined conditions (mean 0.49 day⁻¹) was similar to other strains of *C. acidophila*, which ranged from 0.32 to 0.88 day⁻¹ (Gerloff-Elias et al. 2005; Cuaresma et al. 2006; Tittel et al. 2005). As already reported by several authors, stress promoted by extreme acidity results in high energy

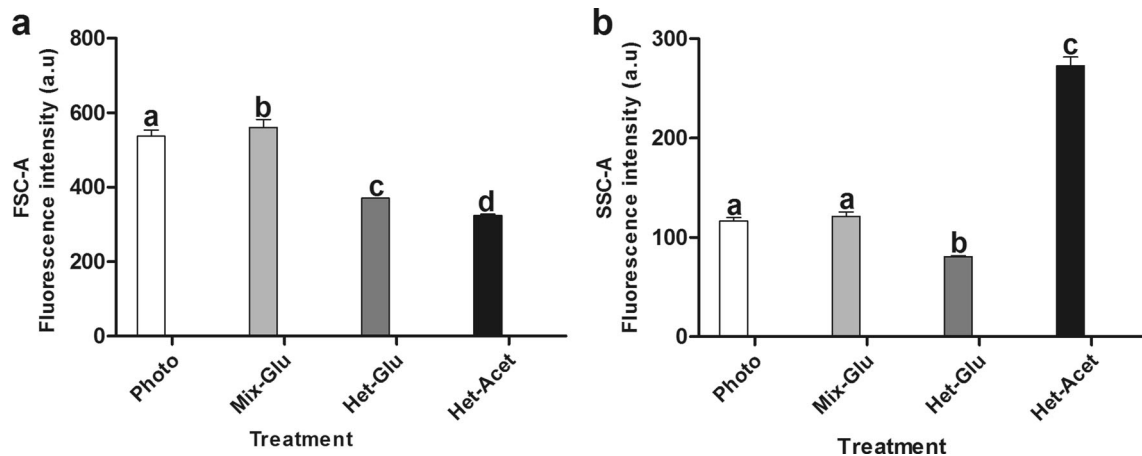


Fig. 4 Flow cytometry of living cells of *C. acidophila* strain LAFIC-004. **a** The FSC-A (fluorescence intensity referring to cell size); **b** SSC-A (fluorescence intensity referring to the cellular complexity); of *C. acidophila*—LAFIC-004 cells in phototrophic (*Photo*) and mixotrophic conditions with 1 % glucose (*Mix-Glu*), mixotrophic with

1 % acetate (*Mix-Acet*), heterotrophic with 1 % glucose (*Het-Glu*), and heterotrophic with 1 % acetate (*Het-Acet*) treatments. The letters indicate significantly different treatments according to the multiple comparison Tukey test (different letters are significantly different at *p* < 0.05) (mean ± SD, *n* = 3)

Fig. 5 Flow cytometry of living cells of *C. acidophila* strain LAFIC-004. Dot plot - cell size (FSC-A) vs. cellular complexity (SSC-A) of *C. acidophila* LAFIC-004 cells in phototrophic (Photo) and mixotrophic conditions with 1 % glucose (Mix-Glu), mixotrophic with 1 % acetate (Mix-Acet), heterotrophic with 1 % glucose (Het-Glu), and heterotrophic with 1 % acetate (Het-Acet) treatments

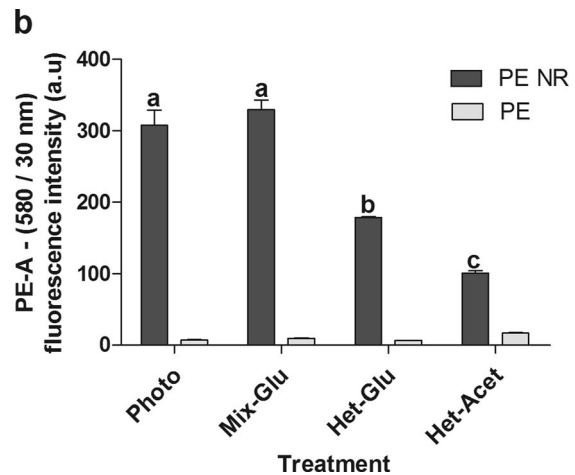
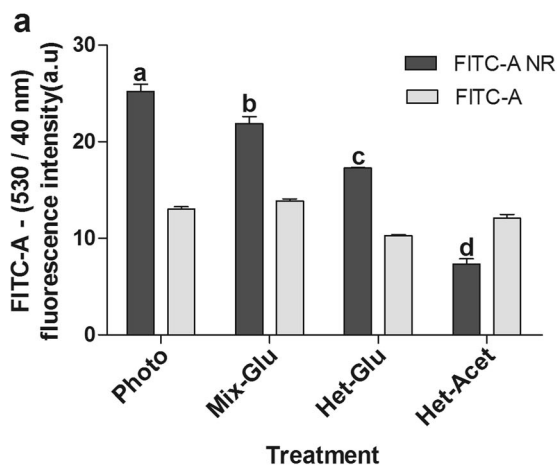
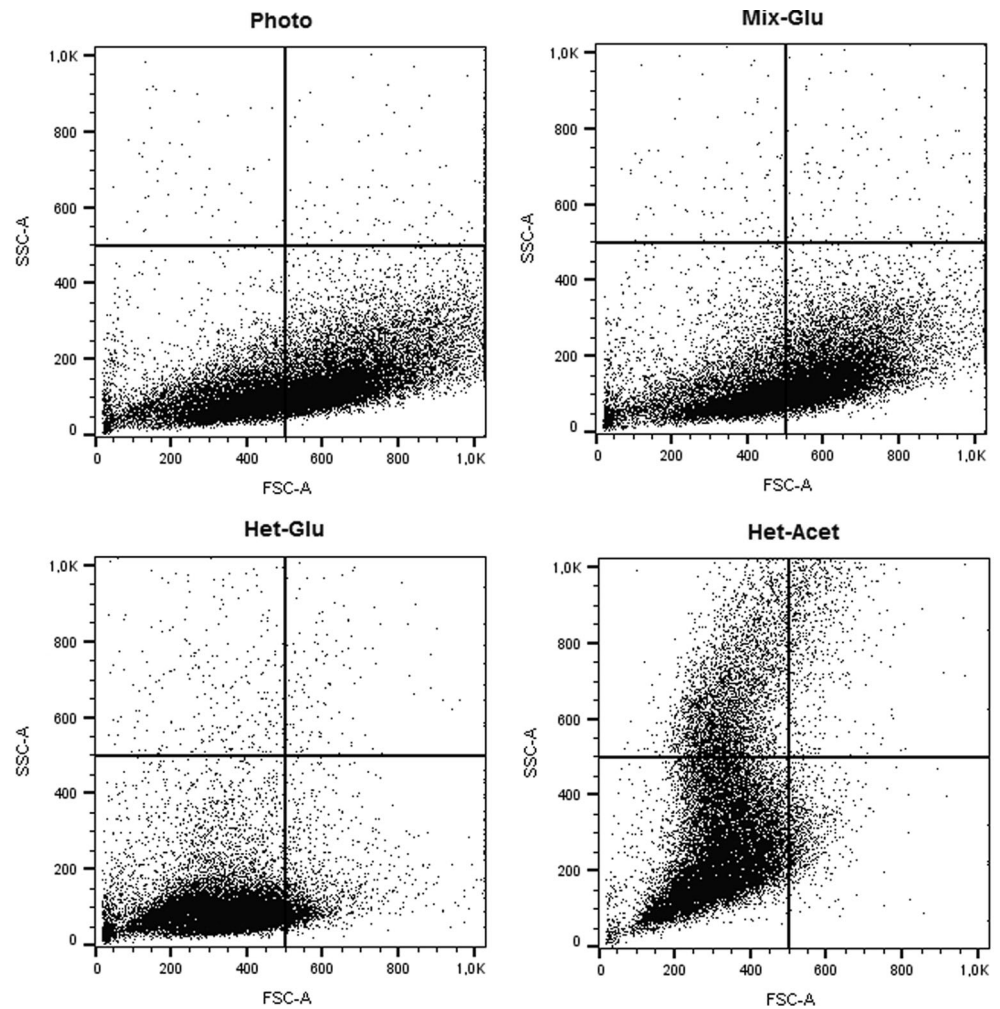
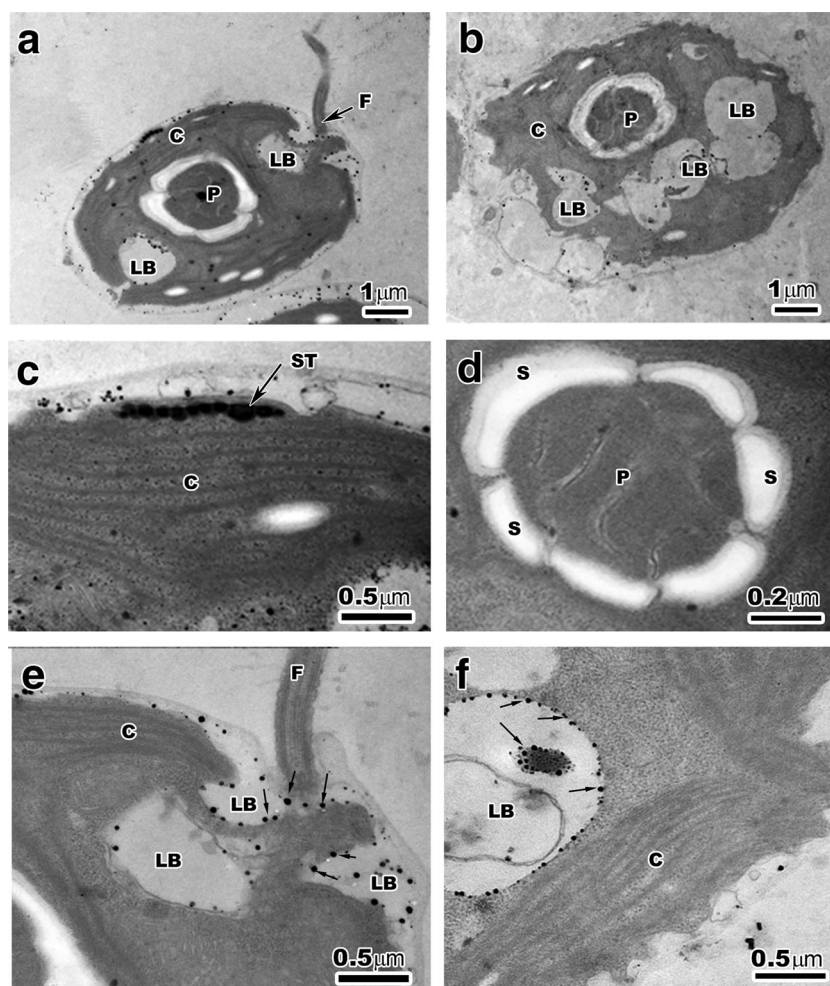


Fig. 6 Flow cytometry of living cells of *C. acidophila* strain LAFIC-004. **a** FITC-A Nile Red (NR) (cells marked with the fluorescence signal NR 530/40 nm), FITC-A (unmarked cells—fluorescence signal 530/40 nm); **(b)** PE-NR (cells marked with the NR—fluorescence signal 580/30 nm—referring to neutral lipids), PE-A (unmarked cells—fluorescence signal 580/30 nm) in the following treatments: phototrophic (*Photo*),

mixotrophic with 1 % glucose (*Mix-Glu*), heterotrophic with 1 % glucose (*Het-Glu*), and heterotrophic with 1 % acetate (*Het-Acet*). The letters indicate significantly different treatments according to the multiple comparison Tukey test (different letters are significantly different at $p < 0.05$) (mean \pm SD, $n = 3$)

Fig. 7 Transmission electron microscopy of *C. acidophila* strain LAFIC-004 grown after 12 days under phototrophic condition. **a, b** Cells show a chloroplast occupying the whole cytoplasmic volume with presence of eyespot (**c**) and pyrenoid (**d**) surrounded by starch grains and various lipid bodies (**e**) with structures inside electron-dense punctuations (*arrows*) (**f**). Chloroplast (**C**), pyrenoid (**P**), lipid bodies (**LB**), starch grains (**S**), flagellum (**F**), eyespot (**E**)



consumption since acidophilic microalgae tend to actively maintain nearly neutral intracellular pH, despite external values (Gerloff-Elias et al. 2005). Moreover, at highly acidic pH, inorganic carbon (CO_2) availability is severely limited (Tittel et al. 2005). Manipulation of culture conditions (irradiance, shaking/aeration, carbon supply) would probably yield higher growth rates. Considering the biotechnological potential of this species in bioremediation (Nishikawa et al. 2003) and lipid production (Langner et al. 2009), alternative culture conditions that enhance this potential and this growth rate can contribute to the viability of commercial applications.

In the present study, we assessed the growth and some physiological and biochemical characteristics of the *C. acidophila* LAFIC-004 strain when cultivated under different conditions (phototrophic, heterotrophic, and mixotrophic), with the use of glucose and acetate as organic carbon sources. Several authors have reported heterotrophic and mixotrophic cultivation modes as good strategies for enhancing growth rates and lipid content in microalgae. Moon et al. (2013) found that *Chlamydomonas reinhardtii* showed higher growth in mixotrophic condition using 1 % acetate, but no growth was reported for this species

under heterotrophic condition. Doebbe et al. (2007) have shown that absorption of glucose in *C. reinhardtii* is limited by the absence of glucose transporters. However, other strains of *C. acidophila* showed satisfactory growth in mixotrophic cultures with glucose (Spijkerman 2007), indicating that the ability to use different sources of organic carbon varies within the genus and even among different strains of the same species. Nevertheless, the higher growth and lipid production for *C. acidophila* LAFIC-004 were observed in phototrophic condition. Cells cultivated under this condition showed integrity and normal intracellular structure. Also, intense chlorophyll *a* fluorescence was detected through confocal microscopy and flow cytometry, indicating high photosynthetic activity.

Cells in the Mix-Glu treatment showed morphophysiological and ultrastructural characteristics similar to those of Photo treatment. The amount of lipid bodies was equivalent, and the population was heterogeneous, showing different cell sizes, but lower growth rate. This lower growth rate is not in accordance with previous studies where *C. acidophila* showed the greatest growth under mixotrophic conditions (Tittel et al. 2005). Heterogeneity in cell population is unquestionably related to

Fig. 8 Transmission electron microscopy of *C. acidophila* strain LAFIC-004 grown after 12 days under mixotrophic treatment with glucose (Mix-Glu) (a, f). Cells with characteristic chloroplast presence of starch grains (a, b), pyrenoid (c), and eyespot (d). Structure of thylakoids in the presence of starch grains (e). Note the increased number of lipid bodies with electron-dense structures (arrows) (f). Chloroplast (C) pyrenoid (P), lipid bodies (LB), starch grains (S), eyespot (E)

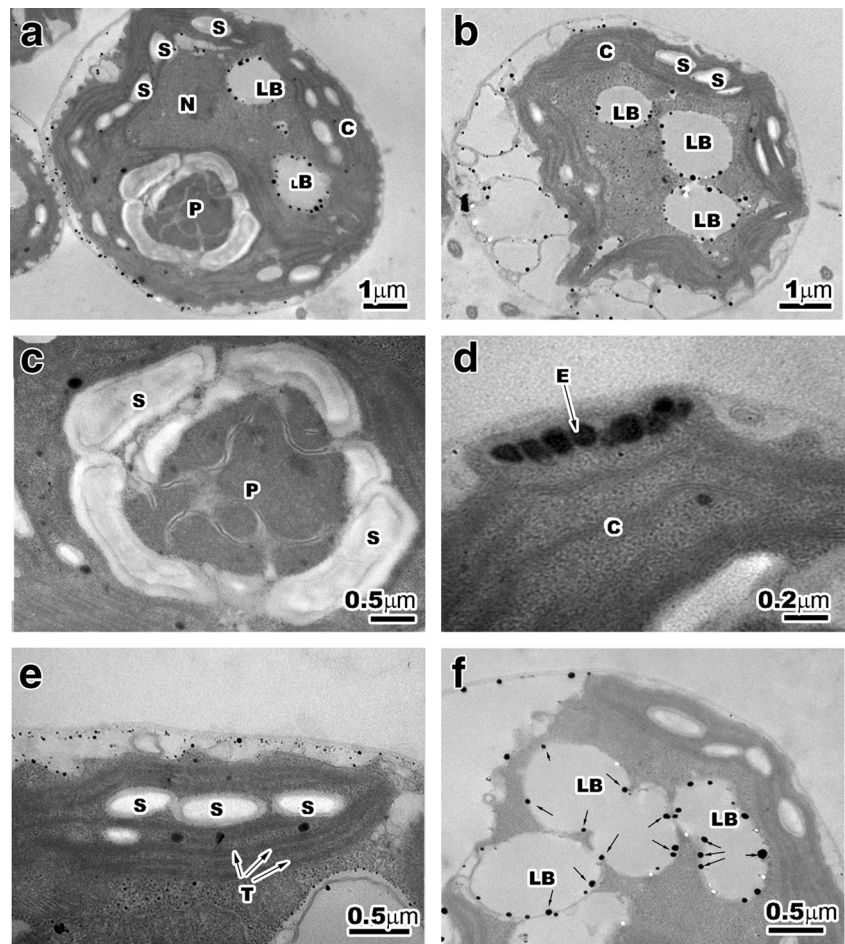


Fig. 9 Transmission electron microscopy of *C. acidophila* strain LAFIC-004 grown after 12 days under heterotrophic treatment with glucose (Het-Glu) (a-d). Cells presenting chloroplast occupying less cell volume, but with characteristic thylakoids (a, b) and pyrenoid with few starch grains and visible thylakoid membranes (c). Lipid bodies are increased by electron-dense punctuations (d). Chloroplast (C) pyrenoid (P), lipid bodies (LB), starch grains (S), eyespot (E)

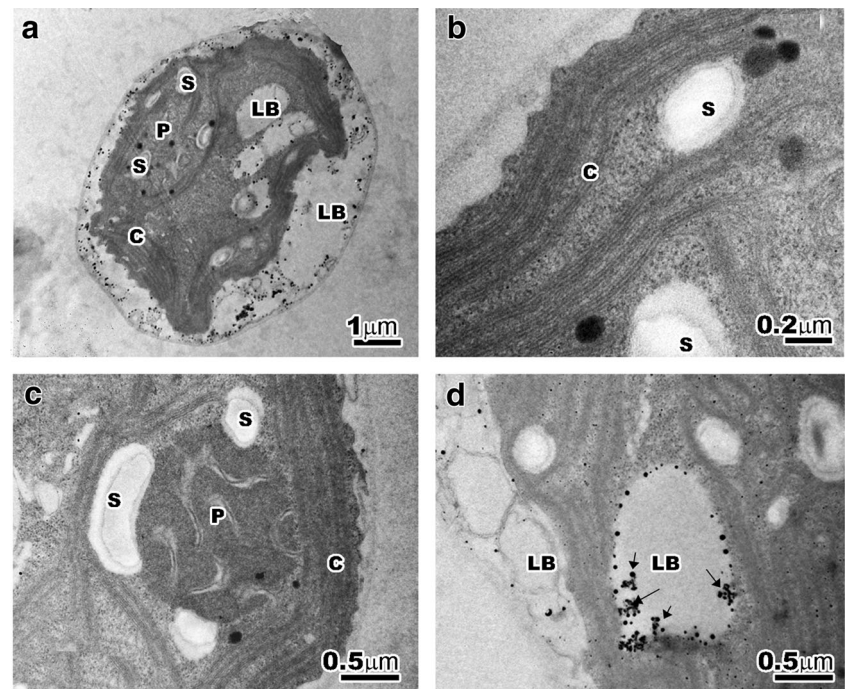
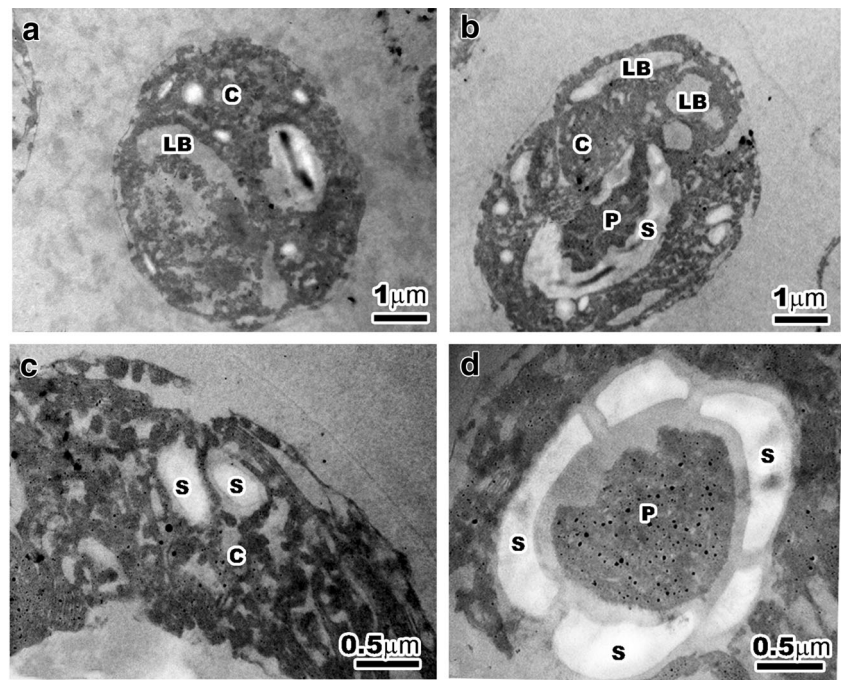


Fig. 10 Transmission electron microscopy of *C. acidophila* strain LAFIC-004 grown after 12 days under heterotrophic treatment with acetate (Het-Acet) (a–d). Cells with altered structure of the chloroplast (a, b). Detail of disintegrated thylakoids (c). Pyrenoid with electron-dense punctuations inside (d). Chloroplast (C), pyrenoid (P), lipid bodies (LB), starch grains (S)



the reproductive cycle of the genus *Chlamydomonas*, which features several cell types with different sizes and structures, including young cells, mature cells, gametes, zygotes, and zoospores (Harris 2009). Sexual reproduction in *Chlamydomonas* spp. is mainly induced by nitrogen starvation. In laboratory cultures, this condition is usually seen at the end of the exponential growth phase, the phase in which cultures of this study were analyzed, both flow cytometry and ultrastructure analysis. Thus, the highest population heterogeneity seen in the Photo and Mix-Glu treatments can be explained by the greater diversity of cell types, resulting from sexual reproduction. In the Het-Glu treatment, in turn, the relative homogeneity of cell population indicates lack of sexual reproduction, probably because of dark condition, since gametogenesis in this genus is dependent on, or, at least, facilitated by, light (Saito et al. 1998).

It is expected that the Mix-Glu treatment would show higher growth rates than Photo treatment since glucose represents an additional source of carbon and energy. This would be especially advantageous in extremely acidic environments as a result of limited CO₂, but this situation has not been verified in our results. We selected three possible explanations for this apparently contradictory result: (a) inability to absorb glucose, (b) regulated growth rate, and (c) unbalanced nutrients in culture media with a high concentration of carbon compared to inorganic nutrients, such as N or P. The first explanation can be refuted, since several studies show that *C. acidophila*, as well as other species of the genus, can absorb and assimilate glucose (Bissinger et al. 2000; Tittel et al. 2005; Spijkerman 2007). Furthermore, the Mix-Glu treatment

showed a greater amount of starch than the Photo treatment, suggesting the participation of glucose in the synthesis of this storage product. This evidence refutes the first explanation.

Regarding the regulation of growth rate, two aspects must be considered. First, this species is extremophilic. Such species are tolerant to environmental extremes and have evolved to grow under one such regime, having virtually no competitors (Seckbach and Oren 2007). This condition eliminates the need for high growth rates by allowing the use of energy for maintenance, rather than growth (e.g., tolerating extreme conditions). Second, the abundance of glucose could reduce the expression of genes (enzymes and transporters) involved in photosynthesis light phase. As a result, in mixotrophic condition, the strain may be growing only, or mainly, by glucose consumption, even in the presence of light. Although this effect of glucose has been reported in a wide range of algae and higher plants (Jang and Sheen 1994), it was not mentioned in other *C. acidophila* mixotrophic growth studies.

The third explanation considers the possibility that reduced growth in mixotrophic condition is associated with high relative concentration of carbon in the medium, e.g., high C/N ratio, from glucose. This may have restricted the otherwise balanced growth of the strain which then responded with a greater accumulation of storage products (starch) in place of growth/reproduction. In fact, the presence of glucose shortens the route of starch synthesis since glucose is directly phosphorylated to glucose-6P and subsequently polymerized, while in the phototrophic pathway with inorganic carbon source (CO₂), the Calvin cycle must occur prior to produce glucose. In this case, supplementation with inorganic nutrients would likely result in higher growth in the Mix-Glu condition.

Studies on the expression of genes related to metabolism are needed for definitive explanations of these issues, which are beyond the scope of the present work.

Under Het-Glu treatment, the cell population was more homogeneous and small in size, exhibiting severe intracellular changes, low pigmentation, and fewer starch granules. This seems to set the stage for low, or no, growth, in turn, threatening survival. It also means that glucose was likely not used as the energy source by this strain in the dark condition. Therefore, survival in this treatment probably resulted from existing intracellular stores. In turn, this suggests that the smaller amount of starch in this treatment could be related to consumption and the inactivation of synthesis as a consequence of the dark condition. The first step of starch synthesis in the plastid is catalyzed by ADPglucose pyrophosphorylase (AGPase), which converts glucose 1-phosphate and ATP to ADP-glucose and PPI, which then initiates the polymerization to starch (Kolbe et al. 2005). The redox activation of AGPase needs the reducing power that comes from the light phase reactions of photosynthesis (Buchanan 1980). This would explain the blockade of synthesis in the absence of light.

Acetate was the carbon source that caused the most pronounced cellular changes. Mix-Acet treatment caused cell death, while under Het-Acet treatment, the cells appeared severely damaged. Pirastru et al. (2012) demonstrated that the growth of the green microalgae *Scenedesmus* sp. in low light with acetate (60–120 mM) showed decreased pigment content concomitant with a decline of electron transport from PSII to PSI. In our study, acetate also affected the photosynthetic activity, as observed by flow cytometry and changes in thylakoids, as observed in TEM images. The disruption of internal membranes clearly indicates acetate toxicity under the tested conditions. This toxicity must be related to the acidic pH of the culture medium used in this study. Chen and Johns (1994; 1996) drew attention to the toxicity of acetate in its undissociated form, which is prevalent in pH under 4.8. These authors reported that concentrations above 0.4 g L⁻¹ acetate inhibited the growth of *C. reinhardtii*. Inhibition of cell growth by acetate occurs by chemical interference with the membrane transport of phosphate, which might result in more expenditure of ATP, causing disruption of cell membranes and changes in cell morphology with the cells becoming irregular and elongated. Moreover, Moon et al. (2013) found that *C. reinhardtii* grew on acetate at higher pH conditions.

Finally, it is important to mention that some microalgae are obligate phototrophs by the lack of transport mechanism for efficient absorption of organic carbon sources. When these transporters are introduced, cells are able to grow heterotrophically (Chen and Chen 2006; Doebbe et al. 2007). However, some microalgae species, such as *Dunaliella tertiolecta* and *Prymnesium parvum*, are unable to assimilate glucose, although having the enzymes needed for its metabolism

(Neilson and Lewin 1974). Similarly, the primary causes of obligate photoautotrophic growth have been attributed to incomplete pathways in the central carbon metabolism, or, perhaps, the absence of enzymatic reaction (Chen and Chen 2006). These findings have led to a greater understanding of microalgae genomics in the last decade (Radakovits et al. 2010), resulting in the publication of genome sequences for some species of microalgae, thus clarifying their metabolic pathways (e.g., Armbrust et al. 2004; Nozaki et al. 2007; Bowler et al. 2008; Blanc et al. 2010; Prochnik et al. 2010). In the case of the strain studied here, evidence suggests no particular lack of these transporters and enzymes.

Lipid analysis of *C. acidophila* LAFIC-004 in phototrophic condition showed 15 % oil content in the exponential phase, which is considered a reasonable result for a strain grown in acidic medium. *Chlamydomonas* spp. yield, in general, around 20 % in lipids by dry weight (DW) (Wang et al. 2009; Work et al. 2010; Mou et al. 2012). When cultures of our strain were kept until late stationary phase, the oil content reached the surprisingly high value of 54 %. This increase was probably related to the lack of inorganic nutrients in the medium, a common phenomenon in stationary phase cultures. In *C. reinhardtii*, the most studied species of the genus, this value tends to increase up to 46 % with nitrogen starvation or in mutants where starch synthesis was inhibited (Wang et al. 2009; Li et al. 2015.). Similar values were obtained with NaCl stress in *Chlamydomonas mexicana* (Salama et al. 2013). These stress conditions can be induced in cultures, or they may be performed in cells taken into stationary growth phase by the tendency to store lipids because of limited nutrients or other resources. Consensus in the literature holds that good lipid-producer microalgae should yield at least 40 % of the dry biomass in lipids (Chisti 2013). To produce high-quality biodiesel, for example, neutral lipids composed of saturated fatty acids, especially C16:0 and C18:0, are desired, with no larger percentage of unsaturated fatty acids than 12 % (Eibl et al. 2014). In *C. acidophila* LAFIC-004, the percentage of saturated fatty acids decreased from 49.12 % in biomass at exponential phase to 33.74 % in biomass at stationary phase. Also, among the unsaturated fatty acids, most were monounsaturated C18:1c (35.7 %) and diunsaturated C18:2 (22.3 %), which does not compromise the quality of oil for use in biodiesel fuel, as would be the case for polyunsaturated fatty acids (Eibl et al. 2014). These lipid data suggest a considerable potential of the strain, either for biodiesel production or other uses. This fact is enhanced if it is taken into consideration that the strain can be grown in wastewater-like acidic drainage from coal mining (AMD), in which the microalgae could most likely perform biosorption of heavy metals, as an additional benefit.

From the results of the present study, it can be concluded that the acidophilic strain *C. acidophila* LAFIC-004 is a good producer of neutral lipids and has a fatty acid profile suitable for biofuel production. The best condition for lipid production

was found to be phototrophic cultivation until late stationary phase. Culture under mixotrophic and heterotrophic conditions with glucose at 1 % did not result in any significant growth increase, and acetate is most likely toxic because of the low pH of the culture medium. Adjustments in inorganic nutrient concentrations may eventually improve the performance of the strain in mixotrophic condition with glucose. Finally, considering that *C. acidophila* LAFIC-004 grows well in acidic and heavy metal-rich wastewater, typical features of acidic mining drainage, a double benefit can be achieved in a future upscale scenario whereby useful biomass is produced, while remediating residues for heavy metals.

Acknowledgments This study was supported by the Coordination for the Improvement of Higher Education Personnel (CAPES, Brazil) and the National Council for Scientific and Technological Development (CNPQ). Luana dos S. Souza has been benefited by a scholarship from CAPES, and this work is part of her PhD thesis. The authors would also like to thank technicians of the Central Laboratory of Electronic Microscopy (LCME) and Multiuser Laboratory of Biology Studies (LAMEB), both from the Federal University of Santa Catarina, Brazil (UFSC).

Authors' contributions All the authors contributed equally to this work.

Compliance with ethical standards

Conflict of interest The authors declare that they have no conflict of interest.

References

- American Oil Chemists' Society (2006) AOCs Official Method Ce 1c-89
- Amburst E, Berges J, Bowler C et al (2004) The genome of the diatom *Thalassiosira pseudonana*: ecology, evolution, and metabolism. *Science* 306:79–86
- Bissinger V, Jander J, Tittel J (2000) A new medium free of organic carbon to cultivate organisms from extremely acidic mining lakes (pH 2.7). *Acta Hydrochim Hydrobiol* 28:310–312
- Blanc G, Duncan G, Agarkova I et al (2010) The *Chlorella variabilis* NC64A genome reveals adaptation to photosymbiosis, coevolution with viruses, and cryptic sex. *Plant Cell* 22:2943–2955
- Bligh EG, Dyer WJ (1959) A rapid method of total lipid extraction and purification. *Can J Biochem Physiol* 37:911–917
- Bouzon ZL, Ouriques LC, Oliveira EC (2005) Ultrastructure of tetraspore germination in the agar-producing seaweed *Gelidium floridanum* (Gelidiales, Rhodophyta). *Phycologia* 44:09–415
- Bowler C, Allen AE, Badger JH et al (2008) The *Phaeodactylum* genome reveals the evolutionary history of diatom genomes. *Nature* 456:239–244
- Buchanan BB (1980) Role of light in the regulation of chloroplast enzymes. *Annu Rev Plant Physiol* 31(341–74):239pp
- Bux F (2013) Biotechnological applications of microalgae: biodiesel and value-added products. CRC Press, Boca Ratón, FL
- Chen GQ, Chen F (2006) Growing phototrophic cells without light. *Biotechnol Lett* 28:607–616
- Chen F, Johns MR (1994) Substrate inhibition of *Chlamydomonas reinhardtii* by acetate in heterotrophic culture. *Process Biochem* 29:245–252
- Chen F, Johns MR (1996) Heterotrophic growth of *Chlamydomonas reinhardtii* on acetate in chemostat culture. *Process Biochem* 31:601–604
- Chisti Y (2007) Biodiesel from microalgae. *Biotechnol Adv* 25:294–306
- Chisti Y (2013) Constraints to commercialization of algal fuels. *J Biotechnol* 167:201–214
- Christie WW (1989) Gas chromatography and lipids—a practical guide, 1 ed, Matreya
- Cirulis JT, Strasser BC, Scott JA, Ross GM (2012) Optimization of staining conditions for microalgae with three lipophilic dyes to reduce precipitation and fluorescence variability. *Cytometry A* 81A:618–662
- Cuaresma M, Garbayo I, Vegab JM, V'ilchez C (2006) Growth and photosynthetic utilization of inorganic carbon of the microalga *Chlamydomonas acidophila* isolated from Tinto River. *Enzyme Microb Technol* 40:158–162
- Doebbe A, Rupprecht J, Beckmanna J, Mussgnuga JH, Hallmann A, Hankamer B, Kruse O (2007) Functional integration of the *HUP1* hexose symporter gene into the genome of *C. reinhardtii*: impacts on biological H₂ production. *J Biotechnol* 131:27–33
- Eibl JK, Corcoran JD, Senhorinho GNA, Zhang K, Hosseini NS, Marsden J, Laamanen CA, Scott JA, Ross GM (2014) Bioprospecting for acidophilic lipid-rich green microalgae isolated from abandoned mine site water bodies. *AMB Express* 4:7
- El-Sayed S, Hyun-Chul K, Abou-ShanabReda AI, Min-Kyu J, You-Kwan O, Seong-Heon K, Byong-Hun J (2013) Biomass, lipid content, and fatty acid composition of freshwater *Chlamydomonas mexicana* and *Scenedesmus obliquus* grown under salt stress. *Bioprocess Biosyst Eng* 36:827–833
- Gerloff-Elias A, Spijkerman E, Pröschold T (2005) Effect of external pH on the growth photosynthesis and photosynthetic electron transport of *Chlamydomonas acidophila* Negoro, isolated from an extremely acidic lake (pH 2.6). *Plant Cell Environ* 28:1218–1229
- Giovanardi M, Ferroni L, Baldissarotto C, Tedeschi P, Maietti A, Pantaleoni L, Pancaldi S (2013) Morphophysiological analyses of *Neochloris oleabundans* (Chlorophyta) grown mixotrophically in a carbon-rich waste product. *Protoplasma* 252:1347–1359
- Guzmán HM, Valido JA, Presmanes KF, Duarte LC (2012) Quick estimation of intraspecific variation of fatty acid composition in *Dunaliella salina* using flow cytometry and Nile Red. *J Appl Phycol* 24:1237–1243
- Harris EH (2009) The *Chlamydomonas* sourcebook—Vol. I: introduction to *Chlamydomonas* and its laboratory use, 2nd edn. Academic Press, Oxford, p 444
- Harwood JL, Jones AL (1989) Lipid metabolism in algae. *Adv Bot Res* 16:1–53
- Inthorn D (2001) Removal of heavy metal by using microalgae. In: Kojima H, Lee YK (eds) Photosynthetic microorganisms in environmental biotechnology. Springer, Hong Kong, pp 111–135
- Jang JC, Sheen J (1994) Sugar sensing in higher plants. *Plant Cell* 6:1665–1679
- Kain JM (1987) Seasonal growth and photoinhibition in *Plocamium cartilagineum* (Rhodophyta) of the Isle of Man. *Phycologia* 26(1):88–99
- Kolbe A, Tiessen A, Schluepmann H, Paul M, Ulrich S, Geigenberger P (2005) Trehalose 6-phosphate regulates starch synthesis via post-translational redox activation of ADP-glucose pyrophosphorylase. *PNAS* 102(31):11118–11123
- Kumar KS, Dahms H-U, Won E-J, Lee J-S, Shin K-H (2015) Microalgae—a promising tool for heavy metal remediation. *Ecotoxicol Environ Saf* 113:329–352
- Langner U, Jakob T, Stehfest K, Wilhelm C (2009) An energy balance from absorbed photons to new biomass for *Chlamydomonas reinhardtii* and *Chlamydomonas acidophila* under neutral and extremely acidic growth conditions. *Plant Cell Environ* 32:250–258
- Lee SJ, Yoon BD, Oh HM (1998) Rapid method for the determination of lipid from the green alga *Botryococcus braunii*. *Biotechnol Tech* 12:553–555

- Li Y, Han D, Hu G, Sommerfeld M, Hu Q (2010) Inhibition of starch synthesis results in overproduction of lipids in *Chlamydomonas reinhardtii*. *Biotechnol Bioeng* 107:258–268
- Li D, Song J-Z, Li H, Shan M-H, Liang Y, Zhu J, Xie Z (2015) Storage lipid synthesis is necessary for autophagy induced by nitrogen starvation. *Febs Lett* 589:269–276
- Liang Y (2013) Producing liquid transportation fuels from heterotrophic microalgae. *Appl Energy* 104:860–868
- Liang YN, Sarkany N, Cui Y (2009) Biomass and lipid productivities of *Chlorella vulgaris* under autotrophic, heterotrophic and mixotrophic growth conditions. *Biotechnol Lett* 31:1043–1049
- Liu J, Huang J, Sun Z, Zhong Y, Jiang Y, Chen F (2011) Differential lipid and fatty acid profiles of photoautotrophic and heterotrophic *Chlorella zofingiensis*: assessment of algal oils for biodiesel production. *Bioresour Technol* 102:106–110
- Liu J, Sun Z, Chen F (2014) Biofuels from algae. *Ed Elsevier* 6:111–142
- Montero MF, Aristizábal M, Reina GG (2011) Isolation of high-lipid content strains of the marine microalga *Tetraselmis suecica* for biodiesel production by flow cytometry and single-cell sorting. *J Appl Phycol* 23:053–1057
- Moon M, Kima C, Park W, Yoo G, Choi Y, Yang J (2013) Mixotrophic growth with acetate or volatile fatty acids maximizes growth and lipid production in *Chlamydomonas reinhardtii*. *Algal Res* 2:352–357
- Mou S, Xu D, Ye N, Zhang X, Liang C, Liang Q, Zheng Z, Zhuang Z, Miao J (2012) Rapid estimation of lipid content in an Antarctic ice alga *Chlamydomonas* using the lipophilic fluorescent dye BODIPY505/515. *J Appl Phycol* 24:1169–1176
- Neilson AH, Lewin RA (1974) The uptake and utilization of organic carbon by algae: an essay in comparative biochemistry. *Phycologia* 13:227–264
- Nishikawa K, Yamakoshi Y, Uemura I, Tominaga N (2003) Ultrastructural changes in *Chlamydomonas acidophila* (Chlorophyta) induced by heavy metals and polyphosphate metabolism. *FEMS Microbiol Ecol* 44:253–259
- Nozaki H, Takano H, Misumi O et al (2007) A 100%-complete sequence reveals unusually simple genomic features in the hostspring red alga *Cyanidioschyzon merolae*. *BMC Biol* 5:1–8
- Olavenson MM, Stoke PM (1989) Responses of the acidophilic alga *Euglena mutabilis* (Euglenophyceae) to carbon enrichment at pH 3. *J Phycol* 25:529–539
- Perez-Garcia O, Bashan Y, Puente ME (2011) Organic carbon supplementation of sterilized municipal wastewater is essential for heterotrophic growth and removing ammonium by the microalga *Chlorella vulgaris*. *J Phycol* 47(1):190–199
- Pirastru L, Darwish M, Chu FL, Perreault F, Sirois L, Sleno L, Popovic R (2012) Carotenoid production and change of photosynthetic functions in *Scenedesmus* sp. exposed to nitrogen limitation and acetate treatment. *J Appl Phycol* 24:117–124
- Přibyl P, Cepák V, Zachleder V (2012) Production of lipids in 10 strains of *Chlorella* and *Parachlorella*, and enhanced lipid productivity in *Chlorella vulgaris*. *Appl Microbiol Biotechnol* 94:540–561
- Prochnik SE, Umen U, Nedelcu AM et al (2010) Genomic analysis of organismal complexity in the multicellular green alga *Volvox carteri*. *Science* 329:223–226
- Radakovits R, Jinkerson RE, Darzins A, Posewitz MC (2010) Genetic engineering of algae for enhanced biofuel production. *Eukaryot Cell* 8:486–50
- Rattapoltee P, Kaewkannetra P (2014) Cultivation of microalga, *Chlorella vulgaris* under different auto-hetero-mixotrophic growths as a raw material during biodiesel production and cost evaluation. *Energy* 78:4–8
- Richmond A, Hu Q (2013) Handbook of microalgal culture: biotechnology and Appl Phycol, 2nd edn. Wiley Blackwell, Oxford, pp 1–736
- Roleda MY, Slocombe SP, Leakey RJG, Day JG, Bell EM, Stanley MS (2013) Effects of temperature and nutrient regimes on biomass and lipid production by six oleaginous microalgae in batch culture employing a two-phase cultivation strategy. *Bioresour Technol* 129:439–449
- Saito T, Inoue M, Yamada M, Matsuda Y (1998) Control of gametic differentiation and activity by light in *Chlamydomonas reinhardtii*. *Plant Cell Physiol* 39:8–15
- Saltpati GG, Pal R (2014) Rapid detection of neutral lipid in green microalgae by flow cytometry in combination with Nile red staining—an improved technique. *Ann Microbiol*. doi:10.1007/s13213-014-0937-5
- Seckbach J, Oren A (2007) Oxygenic photosynthetic microorganisms in extreme environments: possibilities and limitations. In: Seckbach J (ed) *Algae and cyanobacteria in extreme environments*. Springer, The Dordrecht, pp 5–25
- Sharma KK, Schuhmann H, Schenk PM (2012) High lipid induction in microalgae for biodiesel production. *Energies* 5:1532–1553
- Sheehan J, Dunahay T, Benemann J, Roessler P (1998) A look back at the U.S. Department of Energy's Aquatic Species Program—biodiesel from algae. U.S. Department of Energy's Office of Fuels Development. National Renewable Energy Laboratory. NREL/TP-580-24190
- Simioni C, Rover T, Schmidt EC, Felix MRL, Polo LK, Santos R, Costa GB, Kreuzsch M, Pereira DT, Ouriques C, Bouzon ZL (2014) Effects of brefeldin A on the endomembrane system and germ tube formation of the tetraspore of *Gelidium floridanum* (Rhodophyta, Florideophyceae). *J Phycol* 50(3):577–596
- Spijkerman E (2007) Phosphorus acquisition by *Chlamydomonas acidophila* under autotrophic and osmo-mixotrophic growth conditions. *J Exp Bot* 58(15–16):4195–4202
- Spolaore P, Joannis-cassan C, Duran E, Isambert A (2006) Commercial applications of microalgae. *J Biosci Bioeng* 101:87–96
- Tittel J, Bissinger V, Gaedke U, Kamjunke N (2005) Inorganic carbon limitation and mixotrophic growth in *Chlamydomonas* from an acidic mining lake. *Protist* 156:63–75
- Trainor FR (2009) Breaking the habit. Integrating plasticity into taxonomy. *Syst Biodivers* 7:95–100
- USDOE. 2010. National algal biofuels technology roadmap. U.S. Department of Energy, Office of Energy Efficiency and Renewable Energy, Biomass Program. 124p
- Varshney P, Mikulic P, Vonshak A, Beardall J, Wangikar PP (2015) Extremophilic micro-algae and their potential contribution in biotechnology. *Bioresour Technol* 184:363–372
- Velmurugan N, Sung M, Yim SS, Park MS, Yang JW, Jeong KJ (2013) Evaluation of intracellular lipid bodies in *Chlamydomonas reinhardtii* strains by flow cytometry. *Bioresour Technol* 138:30–37
- Wang ZT, Ullrich N, Joo S, Waffenschmidt S, Goodenough U (2009) Algal lipid bodies: stress induction, purification, and biochemical characterization in wild-type and starchless *Chlamydomonas reinhardtii*. *Eukaryotic Cell* 8:1856–1868
- Work VH, Radakovits R, Jinkerson RE, Meuser JE, Elliott LG, Vinyard DJ, Laurens LML, Dismukes GC, Posewitz MC (2010) Increased lipid accumulation in the *Chlamydomonas reinhardtii* sta7-10 starch less Isoamylase mutant and increased carbohydrate synthesis in complemented strains. *Eukaryotic Cell* 9(8):1251–1261
- Wu S, Zhang B, Huang A, Huan L, He L, Lin A, Niu J, Wang G (2014) Detection of intracellular neutral lipid content in the marine microalgae *Proocentrum micans* and *Phaeodactylum tricorutum* using Nile red and BODIPY 505/515. *J Appl Phycol* 26:1659–1668
- Xiong W, Gao C, Yan D, Wu C, Wu Q (2010) Double CO₂ fixation in photosynthesis-fermentation model enhances algal lipid synthesis for biodiesel production. *Bioresour Technol* 101:2287–2293
- Zitta CS, Rover T, Hayashi L, Bouzon ZL (2013) Callus ontogeny of the *Kappaphycus alvarezii* (Rhodophyta, Gigartinales) brown tetrasporophyte strain. *J Appl Phycol* 25:615–629